



# Kent Academic Repository

Bockova, J., Rebelo, A., Ryszka, M., Pandey, R., da Fonseca Cunha, T., Limão-Vieira, P., Mason, Nigel, Pouilly, J.C. and Eden, S. (2019) *Mapping the complex metastable fragmentation pathways of excited 3-aminophenol+*. *International Journal of Mass Spectrometry*, 442 . pp. 95-101. ISSN 1387-3806.

## Downloaded from

<https://kar.kent.ac.uk/74342/> The University of Kent's Academic Repository KAR

## The version of record is available from

<https://doi.org/10.1016/j.ijms.2019.05.006>

## This document version

Author's Accepted Manuscript

## DOI for this version

## Licence for this version

UNSPECIFIED

## Additional information

## Versions of research works

### Versions of Record

If this version is the version of record, it is the same as the published version available on the publisher's web site. Cite as the published version.

### Author Accepted Manuscripts

If this document is identified as the Author Accepted Manuscript it is the version after peer review but before type setting, copy editing or publisher branding. Cite as Surname, Initial. (Year) 'Title of article'. To be published in *Title of Journal* , Volume and issue numbers [peer-reviewed accepted version]. Available at: DOI or URL (Accessed: date).

## Enquiries

If you have questions about this document contact [ResearchSupport@kent.ac.uk](mailto:ResearchSupport@kent.ac.uk). Please include the URL of the record in KAR. If you believe that your, or a third party's rights have been compromised through this document please see our [Take Down policy](https://www.kent.ac.uk/guides/kar-the-kent-academic-repository#policies) (available from <https://www.kent.ac.uk/guides/kar-the-kent-academic-repository#policies>).

# Mapping the complex metastable fragmentation pathways of excited 3-aminophenol<sup>+</sup>

J. Bockova<sup>1</sup>, A. Rebelo<sup>1,2</sup>, M. Ryszka<sup>1</sup>, R. Pandey<sup>1</sup>, T. da Fonseca Cunha<sup>2</sup>, P. Limão-Vieira<sup>2</sup>, N. J. Mason<sup>1,4</sup>, J. C. Pouilly<sup>3</sup>, and S. Eden<sup>1\*</sup>

<sup>1</sup> School of Physical Sciences, The Open University, Walton Hall, Milton Keynes, MK7 6AA, UK

<sup>2</sup> Laboratório de Colisões Atômicas e Moleculares, CEFITEC, Departamento de Física, FCT - Universidade NOVA de Lisboa, P-2829-516 Caparica, Portugal

<sup>3</sup> CEA/CNRS/ENSICAEN/Université de Caen Normandie) Boulevard Becquerel, 14070 Caen, France

<sup>4</sup> School of Physical Sciences, Ingram Building, University of Kent, Canterbury, CT2 7NH, UK

\* Corresponding author: [s.p.eden@open.ac.uk](mailto:s.p.eden@open.ac.uk)

## Abstract

This work applies the technique of mapping ion detection using a reflectron mass spectrometer against flight-time and reflection voltage to elucidate the complex metastable fragmentation pattern of the biomolecular ion 3-aminophenol<sup>+</sup> (3-AP<sup>+</sup>, C<sub>6</sub>H<sub>7</sub>NO<sup>+</sup>). Multi-photon ionization experiments revealed the excited ion's fragmentation routes for the first time and comparisons with calculated flight-times enabled 18 different microsecond-timescale dissociations to be assigned. These included the rare observation of a double hydrogen loss channel from a fragment ion. DFT calculations provided further insights into the most prominent apparent fragmentation sequence: 3-AP<sup>+</sup> (m/z 109) → HCO + C<sub>5</sub>H<sub>6</sub>N<sup>+</sup> (m/z 80) → CNH + C<sub>4</sub>H<sub>5</sub><sup>+</sup> (m/z 53) → C<sub>2</sub>H<sub>2</sub> + C<sub>2</sub>H<sub>3</sub><sup>+</sup> (m/z 27).

## Keywords

Metastable fragmentation; reflectron time-of-flight mass spectrometry; 3-aminophenol; DFT calculations; sequential fragmentation; double hydrogen loss

## 1. Introduction

The dissociation processes of biomolecules, notably the subunits of DNA and proteins, have attracted considerable attention in recent years with the motivation of better understanding the nanoscale mechanisms by which ionizing radiation can initiate damage in biological material [1–4]. Mass spectrometry studies of metastable ions are valuable to identify sequential fragmentation pathways because they simultaneously define ion mass before and after dissociation. Furthermore, metastable dissociation experiments have revealed distinct fragmentation patterns of different molecular isomers [5]. This is of considerable interest because biological function is often highly sensitive to molecular conformation. Metastable dissociation experiments can also provide information on fragment ion energetics, as the microsecond-order time delay implies that the vibrational energy of the precursor ion was very close to the relevant dissociation barrier [6]. Such studies are particularly prevalent in research into the structure and stabilities of molecular clusters [7–12]. This paper showcases the capability of a reflectron mass spectrometry experiment at the Open University (OU) to probe complex metastable fragmentation patterns. The subject of the study is multi-photon ionized 3-aminophenol (3-AP) and the data interpretations are enhanced by DFT calculations.

Aminophenol ( $C_6H_7NO$ ) shares the same phenol group as the amino acid tyrosine and is also closely related to the neurotransmitter dopamine [13]. It is therefore somewhat surprising that the experimental and theoretical work in the literature on the electronic states, ionic states, and fragmentation of 3-AP is extremely sparse. Shinozaki et al. [13] performed resonance enhanced multi-photon ionization (REMPI) experiments on 3-AP in the photon energy range 4.2-4.6 eV, as well as laser induced fluorescence (LIF) measurements and quantum chemical calculations to support their assignments of vibronic structure. 3-AP exists in approximately equal populations of *cis*- and *trans*-conformers in the gas phase [13] and Shinozaki et al.'s REMPI assignments enabled Küpper, Meijer and co-workers to demonstrate the complete separation of these conformers in Stark-deflected pulsed beams [14]. More recently, Yatsyna et al. [15] have performed infrared action spectroscopy measurements on the full set of aminophenol isomers: 2-AP (*cis*- and *trans*-), 3-AP (*cis*- and *trans*-), and 4-AP. The only mass spectra of 3-AP that have been reported are electron impact ionization (EII) measurements [16, 17] and no assignments have been proposed for the fragment ions.

Various mass spectrometry techniques are available to study the metastable dissociation of excited ions, including the post-source decay mode of matrix-assisted laser desorption/ionization (MALDI) [18], double-focusing sector-field [19, 20], and modified linear time-of-flight (TOF) [20, 21]. Reflectron TOF mass spectrometry is also a long-established tool for analyzing metastable dissociation channels [22, 23]. The present reflectron TOF experiments involved measuring multi-photon ionization (MPI) TOF spectra of 3-AP at more than one hundred different reflection voltages. A map comprising all the TOF spectra (with ion flight-time on the x-axis, reflection voltage on the y-axis, and signal intensity color-coded) was then compared with simulated flight-times. This mapping step was invaluable; without it we would not have been able to recognize many of the observed metastable dissociation channels above the detector noise and our assignments would have been less precise. To our knowledge, the earliest paper presenting plots of ion flight-time (or a related parameter such as the *apparent mass* of a metastable peak in a conventional mass spectrum) against reflection voltage to aid assignments was Gilmore and Seah's [24] study of the metastable decay of polytetrafluoroethylene (PTFE) by static secondary-ion mass spectrometry (SIMS). Variations of the mapping approach have subsequently been applied to additional ionized polymers [22], clusters [25–27], and nucleobases [28]. All the previous maps have in common that they show a relatively small number of metastable dissociation channels (maximum 11 [22]) and only one includes a band overlap that can complicate the analysis [25]. The maps presented here for 3-AP<sup>+</sup> enabled 18 metastable dissociation channels to be assigned unambiguously despite four band overlaps.

## 2. Experimental

The experimental system has been described in previous publications [28–30]. Briefly, helium carrier gas (0.5 bar) seeded with sublimated 3-AP (Sigma-Aldrich with stated purity 98%) flowed continuously through a 50  $\mu\text{m}$  diameter pinhole into a pumped chamber ( $500 \text{ ls}^{-1}$ ) to form a supersonic jet. The jet passed through a skimmer into a second pumped chamber and crossed an Nd:YAG-pumped and frequency-doubled dye laser beam (*Continuum Powerlight II 8000 - Sirah Cobra-Stretch*, repetition rate 10 Hz, pulse width 7 ns, pulse energy 100-2,000  $\mu\text{J}$ , wavelength 219-277 nm). The resulting ions were detected using a reflectron time-of-flight (TOF) mass spectrometer (KORE Technology) shown schematically in Fig. 1. The voltage on the reflection electrode can be adjusted to investigate metastable fragmentation. In particular, an ion produced by a dissociation in the *Field-free region* (FFR, 0.4-14.6  $\mu\text{s}$

after the laser pulse) of the mass spectrometer will have relatively low kinetic energy and so can be reflected by a weaker field. The pre-amplified ion signals were timed using a *Fast Comtec P7887* time-to-digital conversion (TDC) card. The data acquisition system was based on a *LabView* application interfacing with the TDC card and a laser pulse energy meter (*Spectrum Detector SPJ-D-8*). A convex lens on a slider was used to control the diameter of the laser beam when it crossed the molecular beam and the average laser pulse energy was adjusted using the delay between the pulses triggering the xenon flash lamps and the *Q-switch* of the Nd:YAG laser.

The 3-AP sublimation temperature in the experiments presented here (Figs. 2-4 and Tables 1-2) was 113 °C. This is lower than 150 °C used in the EII measurement in the AIST database [16] but higher than 80-100 °C used in the previous action spectroscopy experiments [13, 15]. MPI mass spectra were compared in the sublimation temperature range 60-113 °C; no changes in the relative peak heights were observed that could indicate thermally-driven decomposition or reactivity. Similarly, any clustering in the expansion would be expected to depend strongly on the vapour pressure of 3-AP in the nozzle so the fact that the relative peak heights did not change as a function of sublimation temperature suggests that the detected ions did not come from clusters. Background ion signals due to residual gas in the chamber were negligible.

A simulation was developed in Matlab to identify metastable dissociations visible in experimental 2-D maps. The initial inputs are the distances within the mass spectrometer, the electrode voltages (except for the reflection voltage), and the crossing position of the laser beam with the molecular beam. The latter is determined by measuring the *cut-off* reflection voltage at which the intact *parent* ion signal is extinguished, following the method described by Ryszka et al. [30]. The next step is to input one or more *candidate dissociations* (specific combinations of precursor and product ion masses) that might take place in the FFR. The program then generates a map of flight-time against reflection voltage that can be overlaid onto an experimental map. Different candidate dissociations are tested iteratively until a good match is achieved between the simulated and experimental maps (e.g. Fig. 3 (ii) and Fig. 4). The accuracy of the simulation was checked by calculating the flight times of ions traced to *prompt* dissociations (defined here as  $\leq 100$  ns after ionization). The simulated flight-times agree with the experimental TOF spectrum to within  $\leq 0.4\%$ .

### 3. Theoretical method

In order to gain insight into the fragmentation pathways and energetics of the 3-AP radical cation in the gas phase, we have carried out a series of quantum-chemical calculations with density-functional theory on the ionization of the molecule from its neutral electronic ground state at 0 K. All calculations were performed using the Gaussian 09 package [31] with the B3LYP functional (unrestricted spin for radical species in their lowest doublet state) and the aug-cc-pVDZ basis set. This level of theory has been applied widely and successfully for radical cations of organic molecules [32–34] and in particular for the 3-AP radical cation [35]. Geometry optimization was carried out with the default Berny algorithm for both stable species and transition states. Contamination by higher spin states was found to be negligible for all species considered, since the spin operator value was lower than 0.7510 after annihilation. Vibrational frequencies were calculated to confirm the absence of negative frequencies for minima of the potential energy surface, and the presence of a single negative frequency for first-order saddle points. This also allowed the potential energy to be corrected by the vibrational zero-point energy (ZPE).

Only the *cis*- and *trans*-conformers of a single tautomer of 3-AP<sup>+</sup> have been observed previously [35] based on the analysis of vibrational structure up to 0.14 eV above the respective ionization thresholds (7.6205 eV and 7.6544 eV [36]). However, as dissociation clearly necessitates higher internal energies than 0.14 eV, we investigated alternative 3-AP<sup>+</sup> tautomers that could be used as starting points for our fragmentation pathway calculations. All were at least 0.65 eV higher than the tautomer observed by Unterberg et al. [35], with barriers of 2-3 eV between them. Therefore, the calculated pathways start from the lowest-energy tautomer of the radical cation.

### 4. Results and Discussion

Fig. 2 shows an MPI mass spectrum of 3-AP recorded with a reflection voltage (-200 V) that is closer to ground than the cut-off (-254 V) for signals traced to the parent ion and prompt fragment ions. Several features due to metastable dissociation are visible at non-integer *m/z* values but only one (labelled *F* and assigned on the basis of the maps in Fig. 3) has intensity comparable with the prompt fragment ion peaks. The mass spectrum is dominated by 3-AP<sup>+</sup> (with detector saturation), while the strongest fragment ions have *m/z* 80, 39, and 27. This is broadly consistent with the EII mass spectra in the

literature [16, 17] but we recommend against detailed comparisons of peak heights because the present data has not been corrected for kinetic energy release effects on the transmission of different product ions to the detector. Table 1 lists the main prompt fragment ions in Fig. 2; only the peak at  $m/z$  36 ( $C_3^+$ ) is new and may possibly provide indirect evidence for a structural change or dissociation in a neutral excited state [29].

Fig. 3 (i) shows an experimental map of ion counts from multi-photon-ionized 3-AP plotted against flight-time and reflection voltage. The intense bands visible at reflection voltages between -190 and -254 V are due to the detection of prompt fragment ions and 3-AP<sup>+</sup> (consistent with the conventional TOF spectrum in Fig. 2). The curved bands at reflection voltages between -254 and -1,200 V are due to metastable dissociations in the FFR and/or, conceivably, ions dissociating as they scatter off the FFR grids (shown in gold in Fig. 1). To test the latter possible effect, a set of measurements was repeated with two extra grids at the FFR entrance. This doubled the scattering surface but did not change the ratio of *metastable band* signals / prompt ion signals. Therefore, ion interactions with grids had negligible effects on the present data.

TOF measurements carried out at reflection voltage intervals of 10 V are shown in Fig. 3 (i) so the reader can follow individual metastable bands easily. Fig. 3 (ii) shows an equivalent series of measurements with larger voltage intervals (100 V) to enable convenient comparison with the simulations. Table 2 lists the 18 metastable dissociations (labelled A-R) that could be identified on the basis of the agreement between the experimental and simulated maps. Band A ( $m/z$  109  $\rightarrow$  80) has a very broad profile and thus we suspect additional weak contributions of ( $m/z$  109  $\rightarrow$  79) and/or ( $m/z$  109  $\rightarrow$  81) channels.

Aside from showing the agreement of experimental bands with the simulations that determine their assignments, it is worth commenting on how the band shapes in the maps such as Figs. 3-4 can be read in more general terms. To a first approximation, the flight-time at a reflection voltage close to ground (e.g. -200 V) is proportional to  $\frac{1}{2}(\sqrt{m_i} + \sqrt{m_f})$ , where  $m_i$  is the precursor ion mass and  $m_f$  is the product ion mass. Then the ratio of  $\frac{m_f}{m_i}$  determines how far the band extends in reflection voltage (see [28] for the precise relation). A high ratio corresponds to a high kinetic energy of the product ion when it exits the FFR (held at -2,027 V) so a strong electric field is required to reflect it onto the detector. Hence, the

metastable band *cuts-off* at a reflection voltage that is relatively close to ground. The  $\frac{m_f}{m_i}$  ratio also affects the slope of the band on a 2-D map in a given reflection voltage range because the dependence of flight-time on reflection voltage becomes stronger when the ion travels closer to the reflection electrode (thus spending a longer time in the reflecting field).

A *family* of metastable dissociations is suggested by the steady evolution of the shapes of 13 bands in Fig. 3 (A-F, I, K-M, Q, and R). Table 2 shows that these dissociations involve the loss of a neutral comprising two *heavy* atoms (C, N, or O, as well as up to three H atoms). Only two relatively weak bands (G and O) involve the loss of neutrals with three or more heavy atoms and only one band (N) involves the loss of a neutral with a single heavy atom. The remaining two observed bands (H and J) involve double and single H loss. Further experiments and/or calculations are required to explain why metastable channels involving the loss of neutrals comprising two heavy atoms dominate the present results. As a precedent, it is worth noting that the only metastable dissociations observed in EII experiments on the imino tautomer of 2-aminopyrimidine ( $C_4H_5N_3$ , with a  $C_4N_2$  central ring instead of the  $C_6$  ring in 3-AP) were five HCN loss channels and two H loss channels [19].

TOF measurements recorded at reflection voltage intervals of 5 V between -235 and -375 V are presented in Fig. 4 in order to demonstrate metastable single- and double-hydrogen loss from fragment ions. Observations of metastable single-hydrogen loss are quite prevalent in the literature (e.g. from toluene [21] and several derivatives of pyrimidine and purine [19, 37]) even though the similar kinetic energies and flight-times of the precursor and product ions in a TOF mass spectrometer necessitate sensitive measurements and analysis. However, experimental observations of metastable double-hydrogen loss ( $H_2$  or two separate hydrogens) are relatively rare. These channels typically require complex atomic rearrangements, most obviously in the form of *hydrogen scrambling*, and hence pose a challenge to theoretical models of dissociation dynamics. Band J in Fig. 4 corresponds to metastable double hydrogen loss from a fragment ion ( $C_3H_3N^+$  or  $C_4H_5^+$ ). To our knowledge, channels of this kind have only been observed previously from a small selection of pure hydrocarbons with numerous hydrogens [38 and references therein] and from electron impact ionized acrylonitrile ( $C_3H_3N$ ) [39]. Gluch et al. [39] showed that the time dependence of double hydrogen loss from  $C_2H_2^+$  fragments of acrylonitrile can be fitted best using a combination of two separate decay functions and argued that this

suggests H<sub>2</sub> production in stable and unstable states with respect to subsequent dissociation. Other metastable dissociative ionization experiments that provide evidence to distinguish between the production of H<sub>2</sub> or of two separate hydrogens include Feil et al.'s [40] and Roithová et al.'s [41] observations of H<sub>2</sub> loss from doubly-charged toluene. The present experiment does not provide this capability, notably due to the absence of kinetic energy release information.

Our understanding of metastable dissociation is centered on the production of vibrationally hot ions. If the total vibrational energy of an ion matches (or is very close to) the threshold required for a specific dissociation, then a suitable redistribution of the activated modes can lead to delayed dissociation. The delay can be due to tunneling through a low potential barrier or a low rate constant for unimolecular fragmentation when the excess internal energy is small [8]. In contrast with our recent experiments on nucleobases [28], the strongest metastable channels in Fig. 3 involve the delayed dissociation of fragment ions instead of the excited *parent ion*. This suggests that our MPI experiments at 225 nm produced relatively small populations of 3-AP<sup>+</sup> ions in vibrational levels close to a critical dissociation barrier.

The strongest metastable dissociation channel in the present MPI conditions is  $m/z$  80  $\rightarrow$  53 (band F in Fig. 3 (ii)). This appears to be consistent with  $m/z$  80 being the strongest fragment ion in the *prompt mass spectrum* (Fig. 2). Conversely, several quite strong prompt fragment ions (e.g. at  $m/z$  52) are completely absent from the metastable dissociation results, either as precursors or as products. Evidently, some dissociations that take place efficiently on timescales of  $\leq 100$  ns in the present MPI conditions occur too weakly on microsecond timescales to produce discernible metastable dissociation bands. Beyond being the strongest metastable band, the  $m/z$  80  $\rightarrow$  53 channel is interesting because we have also observed metastable dissociations of  $m/z$  109  $\rightarrow$  80 and 53  $\rightarrow$  27. This suggests an unbroken sequential fragmentation route from the excited 3-AP radical cation to one of the smallest fragment ions visible in Figs. 2 and 3. To account for this apparent sequence, we have calculated possible pathways for each channel.

Fig. 5 shows the lowest-energy pathway that we have found for the removal of a 29 a.u. neutral from the lowest-energy tautomer of 3-AP<sup>+</sup>. C<sub>5</sub>H<sub>6</sub>N<sup>+</sup> and HCO are produced by overcoming a barrier of 4.69

eV. Extensive H atom scrambling is observed, which seems to be consistent with the numerous peaks separated by  $m/z$  1 in Fig. 2. Starting from the final  $C_5H_6N^+$  configuration identified in Fig. 5, Fig. 6 shows the lowest-energy pathway that we have found for the loss of a 27 a.u. neutral. This identifies the fragments as  $C_4H_5^+$  and CNH with a critical barrier of 3.49 eV. In the same figure, we also show the lowest energy pathway that we have found for the last step of the apparent fragmentation sequence: the loss of a 26 a.u. neutral from  $C_4H_5^+$ . This results in  $C_2H_3^+$  and  $C_2H_2$  production, overcoming a key barrier of 5.10 eV. Two findings are noticeable: first, the final location of the positive charge corresponds, for each pathway, to the fragment detected experimentally, despite the absence of constraint in the calculation. Second, the relative signals for these three metastable dissociations ( $m/z$  80  $\rightarrow$  53 most intense, then 109  $\rightarrow$  80, then 53  $\rightarrow$  27) correlates with the respective highest energy barriers (3.49, 4.69, and 5.10 eV). Indeed, metastable dissociation is expected to be influenced by rate constants, which depend on potential energy barriers between reactants and products. Future experiments on isotopically-labelled 3-AP and measurements of fragment ion appearance energies would be valuable to test the calculated sequential fragmentation pathway.

## 5. Conclusions

This work reveals a rich array of metastable dissociation channels of a multi-photon ionized aromatic molecule of biological interest: 3-aminophenol. One of the most striking experimental results is the suggestion of a fragmentation sequence which we have assigned to  $3-AP^+ \rightarrow C_5H_6N^+ \rightarrow C_4H_5^+ \rightarrow C_2H_3^+$  on the basis of DFT calculations. Each dissociation in the calculated pathway is preceded by extensive atomic rearrangements, notably hydrogen scrambling. Further evidence supporting hydrogen scrambling is provided by the rare experimental observation of metastable double hydrogen loss ( $H_2$  or two separate atoms) from an excited fragment ion.

## Acknowledgements

The authors are grateful for the expert technical support provided by C. Hall, F. Roberston, R. Seaton, and their colleagues at the Open University (OU). The OU's financial and logistical support is also acknowledged. B. Barc is acknowledged for his role in developing the experimental facility. SE acknowledges the support the British EPSRC through a Life Sciences Interface Fellowship

(EP/E039618/1), a Career Acceleration Fellowship (EP/J002577/1), and a Research Grant (EP/L002191/1). The European Commission is acknowledged for a Marie Curie Intra-European Reintegration Grant (MERC-CT-2007-207292). SE and J-CP are grateful to the CNRS for a PICS grant (07390) supporting the collaboration between CIMAP/GANIL and the OU. TdFC and AR acknowledge the Portuguese National Funding Agency FCT-MCTES through grants SFRH/BD/52538/2014 and PD/BD/114449/2016. This work was supported by Radiation Biology and Biophysics Doctoral Training Programme (RaBBiT, PD/00193/2012); UID/FIS/00068/2019 (CEFITEC); UID/Multi/04378/2013 (UCIBIO). PLV also acknowledges the research grant PTDC/FIS-AQM/31281/2017.

## References

1. Pouilly, J.-C., Vizcaino, V., Schwob, L., Delaunay, R., Kocisek, J., Eden, S., Chesnel, J.-Y., Méry, A., Rangama, J., Adoui, L., Huber, B.: Formation and Fragmentation of Protonated Molecules after Ionization of Amino Acid and Lactic Acid Clusters by Collision with Ions in the Gas Phase. *ChemPhysChem*. 16, 2389–2396 (2015). doi:10.1002/cphc.201500275
2. Matsika, S., Spanner, M., Kotur, M., Weinacht, T.C.: Ultrafast Relaxation Dynamics of Uracil Probed via Strong Field Dissociative Ionization. *J. Phys. Chem. A*. 117, 12796–12801 (2013). doi:10.1021/jp408073d
3. Fabrikant, I.I., Eden, S., Mason, N.J., Fedor, J.: Recent Progress in Dissociative Electron Attachment: From Diatomics to Biomolecules. Academic Press, Burlington (2017)
4. Milosavljević, A.R., Cerovski, V.Z., Canon, F., Ranković, M.L., Škoro, N., Nahon, L., Giuliani, A.: Energy-Dependent UV Photodissociation of Gas-Phase Adenosine Monophosphate Nucleotide Ions: The Role of a Single Solvent Molecule. *J. Phys. Chem. Lett.* 5, 1994–1999 (2014). doi:10.1021/jz500696b
5. Shannon, T.W., McLafferty, F.W.: Identification of Gaseous Organic Ions by the Use of “Metastable Peaks”<sup>1</sup>. *J. Am. Chem. Soc.* 88, 5021–5022 (1966). doi:10.1021/ja00973a045
6. Pandey, R., Lalande, M., Ryszka, M., Limão-Vieira, P., Mason, N.J., Pouilly, J.C., Eden, S.: Stabilities of nanohydrated thymine radical cations: insights from multi-photon ionization experiments and ab initio calculations. *Eur. Phys. J. D*. 71, 1–8 (2017). doi:10.1140/epjd/e2017-70827-1

7. Continetti, R.E.: Photoelectron-photofragment coincidence studies of dissociation dynamics. *Int. Rev. Phys. Chem.* 17, 227–260 (1998). doi:10.1080/014423598230144
8. Cooks, R.G., Beynon, J.H., Caprioli, R.M., Lester, G.R.: *Metastable Ions*. Elsevier, Amsterdam (1973)
9. Feil, S., Gluch, K., Denifl, S., Zappa, F., Echt, O., Scheier, P., Märk, T.D.: Metastable dissociation and kinetic energy release of helium clusters upon electron impact ionization. *Int. J. Mass Spectrom.* 252, 166–172 (2006). doi:10.1016/j.ijms.2006.01.055
10. Ishiuchi, S., Sakai, M., Daigoku, K., Hashimoto, K., Fujii, M.: Hydrogen transfer dynamics in a photoexcited phenol/ammonia (1 : 3) cluster studied by picosecond time-resolved UV-IR-UV ion dip spectroscopy. *J. Chem. Phys.* 127, 234304 (2007). doi:10.1063/1.2806182
11. Kim, N.J., Kim, Y.S., Jeong, G., Ahn, T.K., Kim, S.K.: Hydration of DNA base cations in the gas phase. *Int. J. Mass Spectrom.* 219, 11–21 (2002). doi:10.1016/S1387-3806(02)00547-X
12. Bruzzi, E., Raggi, G., Parajuli, R., Stace, A.J.: Experimental Binding Energies for the Metal Complexes  $[Mg(NH_3)_n]^{2+}$ ,  $[Ca(NH_3)_n]^{2+}$ , and  $[Sr(NH_3)_n]^{2+}$  for  $n = 4–20$  Determined from Kinetic Energy Release Measurements. *J. Phys. Chem. A.* 118, 8525–8532 (2014). doi:10.1021/jp5022642
13. Shinozaki, M., Sakai, M., Yamaguchi, S., Fujioka, T., Fujii, M.:  $S_1–S_0$  Electronic spectrum of jet-cooled *m*-aminophenol. *Phys. Chem. Chem. Phys.* 5, 5044–5050 (2003). doi:10.1039/B309461H
14. Filsinger, F., Küpper, J., Meijer, G., Hansen, J.L., Maurer, J., Nielsen, J.H., Holmegaard, L., Stapelfeldt, H.: Pure Samples of Individual Conformers: The Separation of Stereoisomers of Complex Molecules Using Electric Fields. *Angew. Chemie Int. Ed.* 48, 6900–6902 (2009). doi:10.1002/anie.200902650
15. Yatsyna, V., Bakker, D.J., Feifel, R., Rijs, A.M., Zhaunerchyk, V.: Aminophenol isomers unraveled by conformer-specific far-IR action spectroscopy. *Phys. Chem. Chem. Phys.* 18, 6275–6283 (2016). doi:10.1039/c5cp07426f
16. National Institute of Advanced Industrial Science and Technology (AIST): Spectral Database For Organic Compounds SDBS, <https://sdb.sdb.aist.go.jp/sdb/cgi-bin/landingpage?sdbno=1514>
17. National Institute of Standards and Technology (NIST): 3-aminophenol, <https://webbook.nist.gov/cgi/cbook.cgi?ID=C591275&Mask=200#Mass-Spec>
18. Bald, I., Flosadóttir, H.D., Ómarsson, B., Ingólfsson, O.: Metastable fragmentation of a thymidine-

- nucleotide and its components. *Int. J. Mass Spectrom.* 313, 15–20 (2012). doi:10.1016/j.ijms.2011.12.007
19. Rice, J.M., Dudek, G.O., Barber, M.: Mass Spectra of Nucleic Acid Derivatives. Pyrimidines. *J. Am. Chem. Soc.* 87, 4569–4576 (1965). doi:10.1021/ja00948a029
  20. Mauracher, A., Denifl, S., Edtbauer, A., Hager, M., Probst, M., Echt, O., Märk, T.D., Scheier, P., Field, T.A., Graupner, K.: Metastable anions of dinitrobenzene: Resonances for electron attachment and kinetic energy release. *J. Chem. Phys.* 133, 244302 (2010). doi:10.1063/1.3514931
  21. Haddon, W.F., McLafferty, F.W.: Metastable Ion Characteristics. Measurements with a Modified Time-of-Flight Mass Spectrometer. *Anal. Chem.* 41, 31–36 (1969). doi:10.1021/ac60270a006
  22. Shard, A.G., Gilmore, I.S.: Analysis of metastable ions in the ToF-SIMS spectra of polymers. *Int. J. Mass Spectrom.* 269, 85–94 (2008). doi:10.1016/j.ijms.2007.09.011
  23. L'Hermite, J.M., Rabilloud, F., Labastie, P., Spiegelman, F.: Evidence for trimers evaporation in silver bromide clusters. *Eur. Phys. J. D.* 16, 77–80 (2001). doi:10.1007/s100530170064
  24. Gilmore, I.S., Seah, M.P.: Static SIMS: Metastable decay and peak intensities. *Appl. Surf. Sci.* 144–145, 26–30 (1999). doi:10.1016/S0169-4332(98)00757-0
  25. L'Hermite, J.M., Marcou, L., Rabilloud, F., Labastie, P.: A new method to study metastable fragmentation of clusters using a reflectron time-of-flight mass spectrometer. *Rev. Sci. Instrum.* 71, 2033–2037 (2000). doi:10.1063/1.1150573
  26. L'Hermite, J.M., Rabilloud, F., Marcou, L., Labastie, P.: Metastable fragmentation of silver bromide clusters. *Eur. Phys. J. D.* 14, 323–330 (2001). doi:10.1007/s100530170199
  27. Ponciano, C.R., Ávalos, F.E., Rentería, A., Da Silveira, E.F.: Analysis of metastable decay by time-of-flight coincidence and kinetics energy measurements. *Int. J. Mass Spectrom.* 209, 197–208 (2001). doi:10.1016/S1387-3806(01)00496-1
  28. Pandey, R., Ryszka, M., da Fonseca Cunha, T., Lalande, M., Dampc, M., Limão-Vieira, P., Mason, N.J., Pouilly, J.C., Eden, S.: Threshold behavior in metastable dissociation of multi-photon ionized thymine and uracil. *Chem. Phys. Lett.* 684, 233–238 (2017). doi:10.1016/j.cplett.2017.06.051
  29. Barc, B., Ryszka, M., Spurrell, J., Dampc, M., Limão-Vieira, P., Parajuli, R., Mason, N.J., Eden, S.: Multi-photon ionization and fragmentation of uracil: Neutral excited-state ring opening and

- hydration effects. *J. Chem. Phys.* 139, 244311 (2013). doi:10.1063/1.4851476
30. Ryszka, M., Pandey, R., Rizk, C., Tabet, J., Barc, B., Dampc, M., Mason, N.J., Eden, S.: Dissociative multi-photon ionization of isolated uracil and uracil-adenine complexes. *Int. J. Mass Spectrom.* 396, 48–54 (2016). doi:10.1016/j.ijms.2015.12.006
31. Frisch, M.J., Trucks, G.W., Schlegel, H.B., Scuseria, G.E., Robb, M.A., Cheeseman, J.R., Scalmani, G., Barone, V., Petersson, G.A., Nakatsuji, H., Li, X., Caricato, M., Marenich, A., Bloino, J., Janesko, B.G., Gomperts, R., Mennucci, B., Hratchian, H.P., Ortiz, J. V., Izmaylov, A.F., Sonnenberg, J.L., Williams-Young, D., Ding, F., Lipparini, F., Egidi, F., Goings, J., Peng, B., Petrone, A., Henderson, T., Ranasinghe, D., Zakrzewski, V.G., Gao, J., Rega, N., Zheng, G., Liang, W., Hada, M., Ehara, M., Toyota, K., Fukuda, R., Hasegawa, J., Ishida, M., Nakajima, T., Honda, Y., Kitao, O., Nakai, H., Vreven, T., Throssell, K., J. A. Montgomery, J., Peralta, J.E., Ogliaro, F., Bearpark, M., Heyd, J.J., Brothers, E., Kudin, K.N., Staroverov, V.N., Keith, T., Kobayashi, R., Normand, J., Raghavachari, K., Rendell, A., Burant, J.C., Iyengar, S.S., Tomasi, J., Cossi, M., Millam, J.M., Klene, M., Adamo, C., Cammi, R., Ochterski, J.W., Martin, R.L., Morokuma, K., Farkas, O., Foresman, J.B., Fox, D.J.: *Gaussian 09, Revision A.02*. Gaussian, Inc., Wallingford (2016)
32. Sodupe, M., Oliva, A., Bertran, J.: Theoretical study of the ionization of phenol-water and phenol-ammonia hydrogen-bonded complexes. *J. Phys. Chem. A.* 101, 9142–9151 (1997). doi:10.1021/jp970571m
33. Bertran, J., Oliva, A., Rodriguez-Santiago, L., Sodupe, M.: Single versus double proton-transfer reactions in Watson-Crick base pair radical cations. A theoretical study. *J. Am. Chem. Soc.* 120, 8159–8167 (1998). doi:10.1021/ja9804417
34. Kumar, A., Sevilla, M.D.: Influence of Hydration on Proton Transfer in the Guanine-Cytosine Radical Cation (G( $\cdot+$ )-C) Base Pair: A Density Functional Theory Study. *J. Phys. Chem. B.* 113, 11359–11361 (2009). doi:10.1021/jp903403d
35. Unterberg, C., Gerlach, A., Jansen, A., Gerhards, M.: Structures and vibrations of neutral and cationic 3-and 4-aminophenol. *Chem. Phys.* 304, 237–244 (2004). doi:10.1016/j.chemphys.2004.06.036
36. Sohn, W.Y., Kim, M., Kim, S.-S., Park, Y.D., Kang, H.: Solvent-assisted conformational isomerization and the conformationally-pure REMPI spectrum of 3-aminophenol. *Phys. Chem.*

- Chem. Phys. 13, 7037 (2011). doi:10.1039/c0cp02592e
37. Rice, J.M., Dudek, G.: Mass Spectra of Nucleic Acid Derivatives. II. Guanine, Adenine, and Related Compounds. *J. Am. Chem. Soc.* 89, 2719–2725 (1966). doi:10.1021/ja00987a039
  38. Ottinger, C.: Metastable Ions in the Mass Spectra of Propane and Deuterated Propanes. *J. Chem. Phys.* 47, 1452–1457 (1967). doi:10.1063/1.1712101
  39. Głuch, K., Szot, E., Gruszecka, A., Szymańska-Chargot, M., Cytawa, J., Michalak, L.: Kinetic energy release and mean life time of metastable ions produced from C<sub>3</sub>H<sub>3</sub>N. *Vacuum.* 83, S20–S23 (2009). doi:10.1016/j.vacuum.2009.01.014
  40. Feil, S., Echt, O., Głuch, K., Hasan, V.G., Matt-Leubner, S., Tepnual, T., Grill, V., Bacher, A., Scheier, P., Märk, T.D.: Metastable dissociation of doubly charged ions produced from toluene: Kinetic energy release upon charge separation and H<sub>2</sub>elimination. *Chem. Phys. Lett.* 411, 366–372 (2005). doi:10.1016/j.cplett.2005.06.051
  41. Roithová, J., Schröder, D., Gruene, P., Weiske, T., Schwarz, H.: Structural aspects of long-lived C<sub>7</sub>H<sub>8</sub><sup>2+</sup> dications generated by the electron ionization of toluene. *J. Phys. Chem. A.* 110, 2970–2978 (2006). doi:10.1021/jp0545288

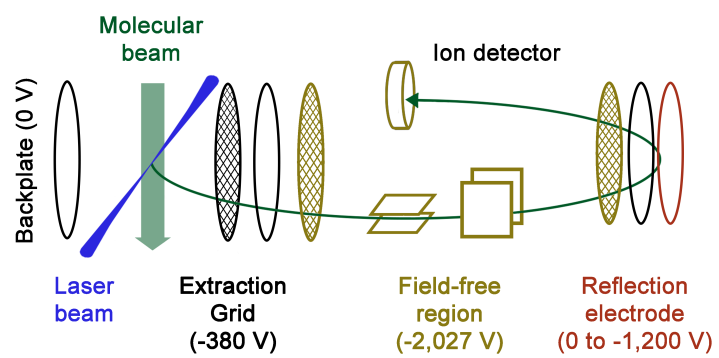


**Fig. 1:** Schematic diagram of the reflectron TOF mass spectrometer.

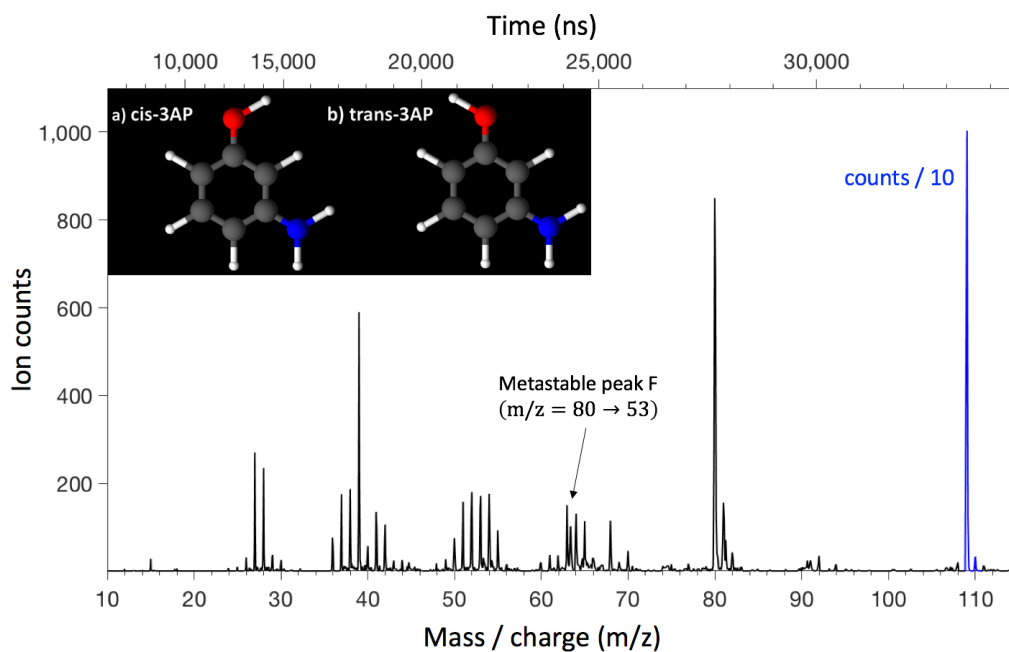


**Fig. 2:** MPI mass spectrum of 3-AP (225 nm, average UV laser fluence  $3 \times 10^7 \text{ W} \cdot \text{cm}^{-2}$ , reflection voltage -200 V). Inserts (a) and (b) represent the structures of the *cis*- and *trans*-conformers of neutral 3-AP in the electronic ground state. Our calculated lowest-energy geometries of the *cis*- and *trans*-conformers of 3-AP<sup>+</sup> (not shown here for brevity) are very close to the corresponding neutrals.

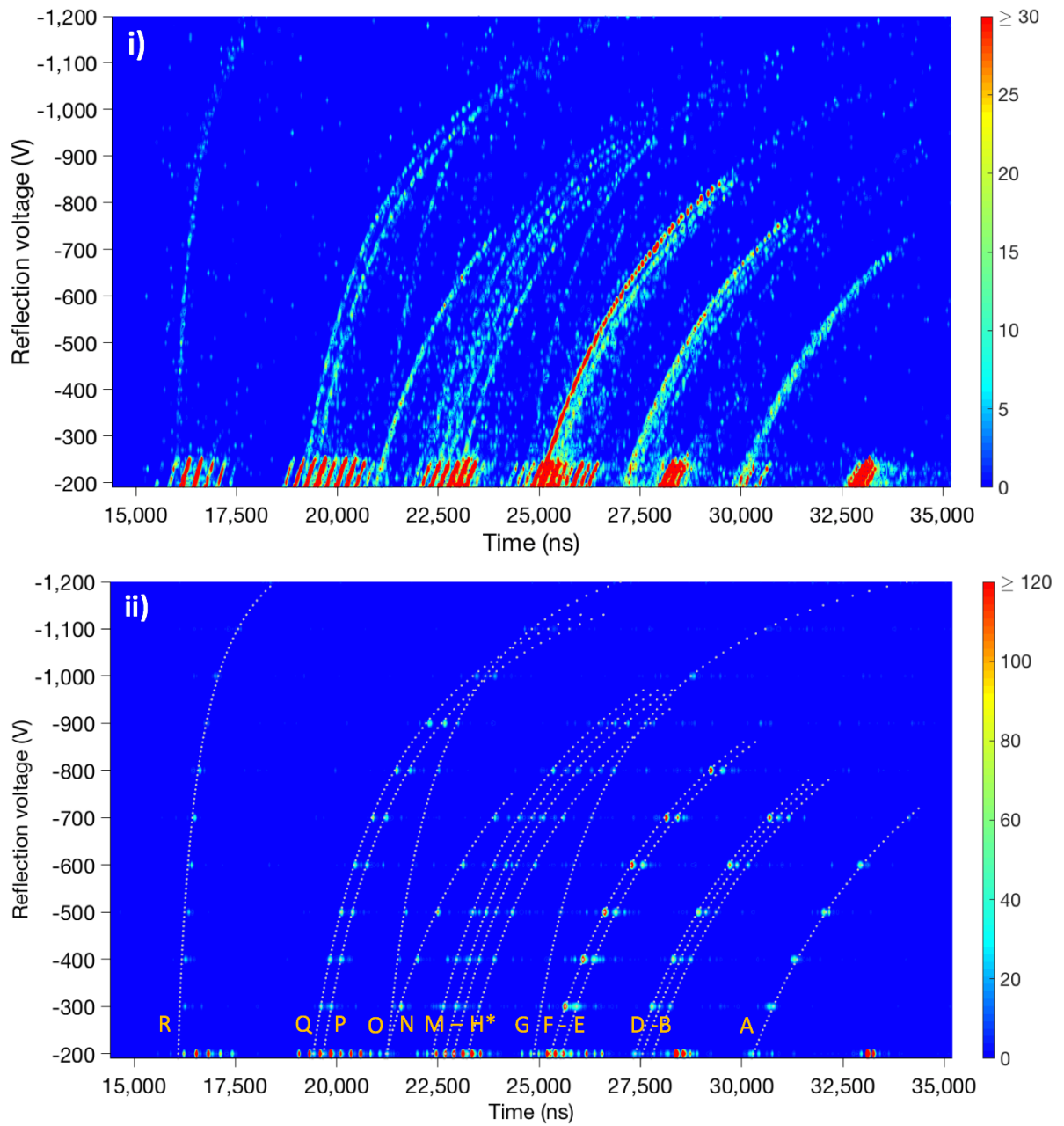


**Fig. 3:** (i) Experimental map of MPI signal (225 nm, average fluence  $3 \times 10^7 \text{ W.cm}^{-2}$ ) against flight-time and reflection voltage. (ii) Superposition of experimental and simulated maps, with the simulated bands shown as dotted white lines. The scales on the right-hand side of the maps are in ion counts per 32 ns time bin. \* Bands H and J are shown in detail in Fig. 4.

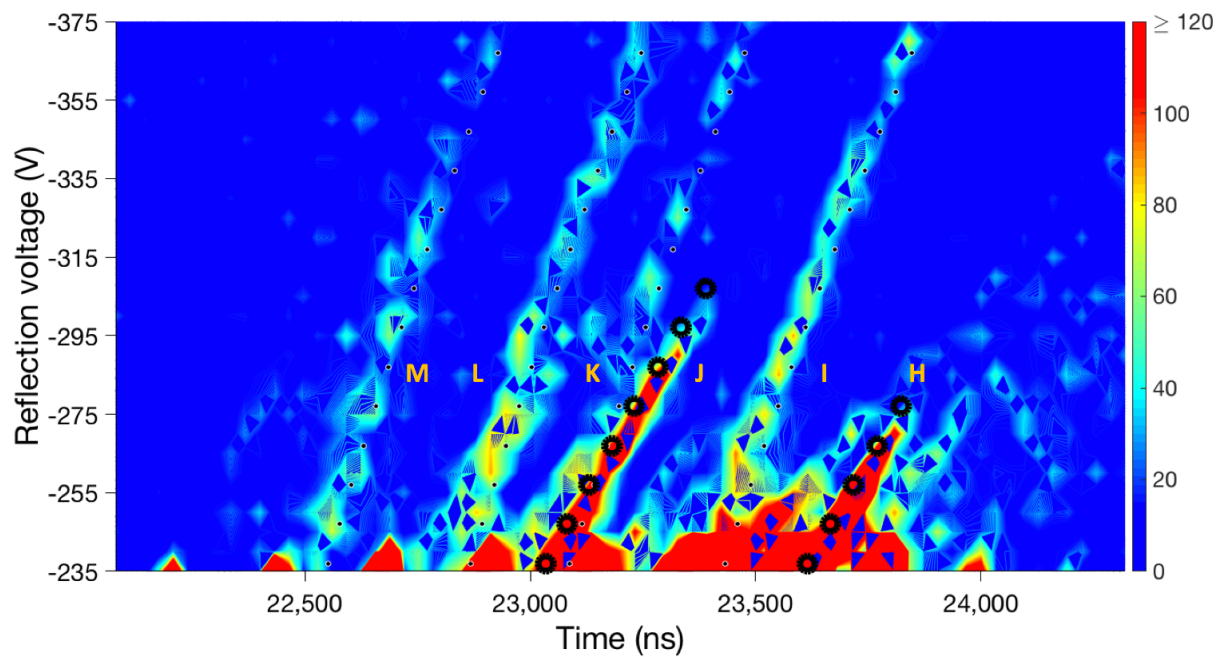


**Fig. 4:** Detail of the experimental map of MPI signal (225 nm, average fluence  $3 \times 10^7 \text{ W.cm}^{-2}$ ) against flight-time and reflection voltage. The simulated bands for  $m/z$  55  $\rightarrow$  54 and 53  $\rightarrow$  51 metastable dissociations (involving single- and double-hydrogen loss) are indicated by open black circles and agree closely with the experimental H and J bands, respectively. The scale on the right-hand side of the map is in ion counts per 32 ns time bin.

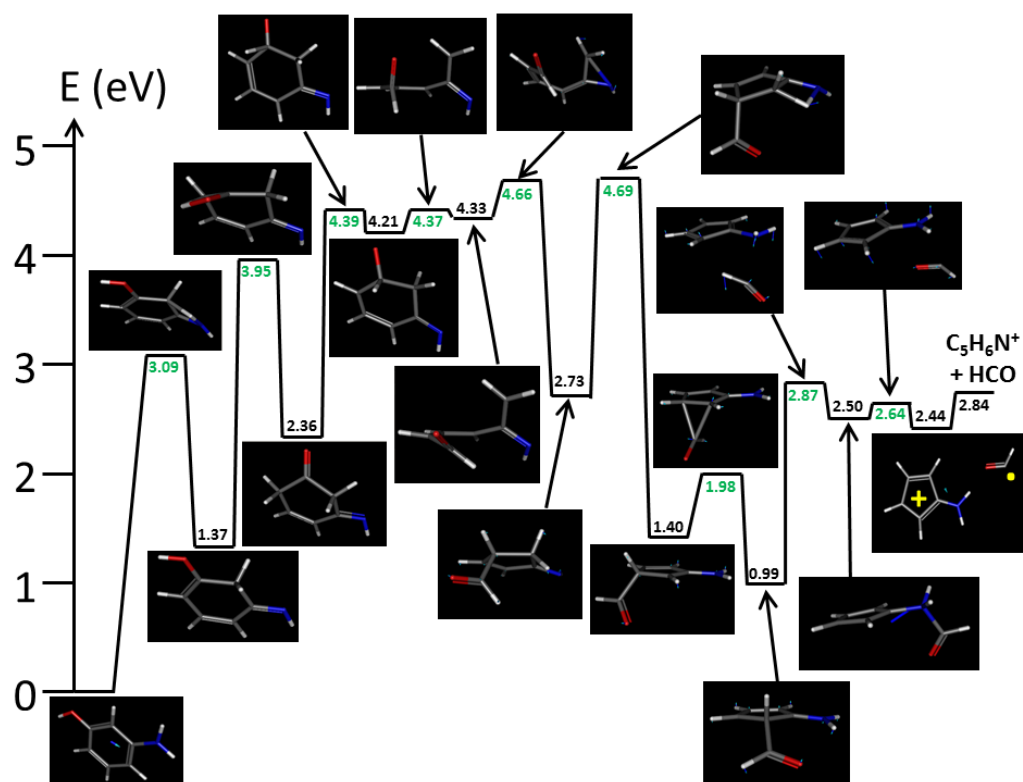


**Fig. 5.** Potential energy surface along HCO loss from 3-AP<sup>+</sup> ( $m/z$  109  $\rightarrow$  80, band A in Fig. 3). The zero-point corrected energy of the doublet ground-state of each species (in black for minima and green for transition states) is given in eV, relative to that of the lowest-energy tautomer. The structure of each species is also shown: H atoms are colored in white, C in grey, O in red and N in blue. The locations of the positive charge and the radical are indicated in yellow for the last minimum before fragmentation.

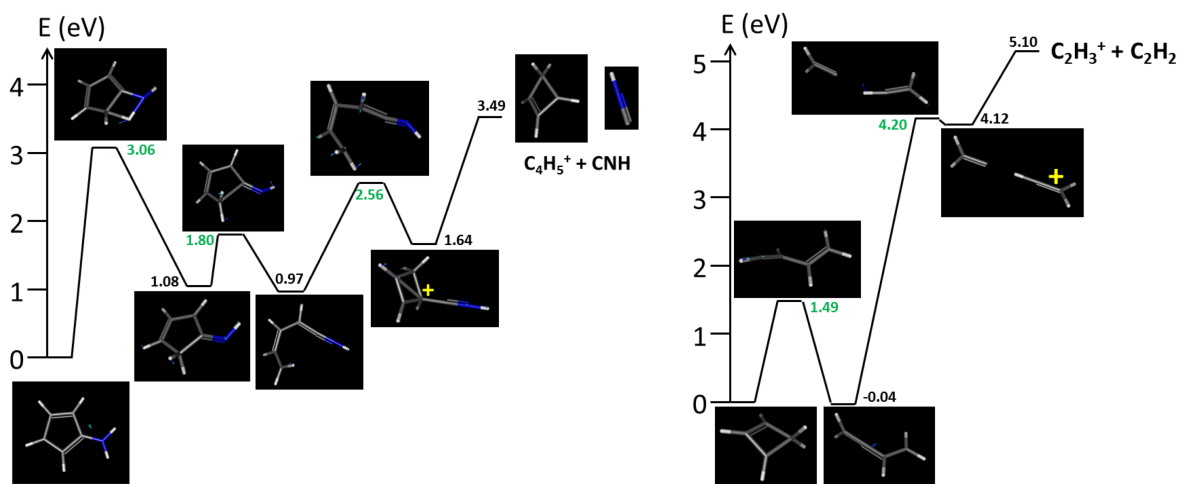


**Fig. 6.** Potential energy surfaces along (left) CNH loss from  $C_5H_6N^+$  ( $m/z$  80  $\rightarrow$  53, band F) and (right)  $C_2H_2$  loss from  $C_4H_5^+$  ( $m/z$  53  $\rightarrow$  27, band Q). See the Fig. 5 caption for further details.

**Table 1:** Summary of the prompt fragment ion signals in Fig. 2.

m/z <sup>a</sup>	Plausible product ions <sup>b</sup>
109 <sup>c</sup>	3-AP <sup>+</sup> (C <sub>6</sub> H <sub>7</sub> NO <sup>+</sup> )
80 <sup>cd</sup>	<b>C<sub>5</sub>H<sub>6</sub>N<sup>+</sup></b>
68 <sup>c</sup>	C <sub>3</sub> H <sub>2</sub> NO <sup>+</sup> / C <sub>4</sub> H <sub>6</sub> N <sup>+</sup> / C <sub>4</sub> H <sub>4</sub> O <sup>+</sup>
66 <sup>cd</sup>	C <sub>4</sub> H <sub>4</sub> N <sup>+</sup> / C <sub>4</sub> H <sub>2</sub> O <sup>+</sup> / C <sub>5</sub> H <sub>6</sub> <sup>+</sup> / C <sub>3</sub> NO <sup>+</sup>
65 <sup>d</sup>	C <sub>4</sub> H <sub>3</sub> N <sup>+</sup> / C <sub>5</sub> H <sub>5</sub> <sup>+</sup>
64 <sup>d</sup>	C <sub>4</sub> H <sub>2</sub> N <sup>+</sup> / C <sub>5</sub> H <sub>4</sub> <sup>+</sup>
63	C <sub>4</sub> HN <sup>+</sup> / C <sub>5</sub> H <sub>3</sub> <sup>+</sup>
55 <sup>c</sup>	C <sub>2</sub> HNO <sup>+</sup> / C <sub>3</sub> H <sub>5</sub> N <sup>+</sup> / C <sub>4</sub> H <sub>7</sub> <sup>+</sup> / C <sub>3</sub> H <sub>3</sub> O <sup>+</sup>
54 <sup>ccdd</sup>	C <sub>3</sub> H <sub>4</sub> N <sup>+</sup> / C <sub>3</sub> H <sub>2</sub> O <sup>+</sup> / C <sub>4</sub> H <sub>6</sub> <sup>+</sup> / C <sub>2</sub> NO <sup>+</sup>
53 <sup>ccd</sup>	<b>C<sub>4</sub>H<sub>5</sub><sup>+</sup></b>
52	C <sub>3</sub> H <sub>2</sub> N <sup>+</sup> / C <sub>4</sub> H <sub>4</sub> <sup>+</sup>
51 <sup>d</sup>	C <sub>3</sub> HN <sup>+</sup> / C <sub>4</sub> H <sub>3</sub> <sup>+</sup>
50	C <sub>4</sub> H <sub>2</sub> <sup>+</sup> / C <sub>3</sub> N <sup>+</sup>
42	C <sub>2</sub> H <sub>4</sub> N <sup>+</sup> / C <sub>2</sub> H <sub>2</sub> O <sup>+</sup> / C <sub>3</sub> H <sub>6</sub> <sup>+</sup> / CNO <sup>+</sup>
41 <sup>cdd</sup>	C <sub>2</sub> H <sub>3</sub> N <sup>+</sup> / C <sub>2</sub> HO <sup>+</sup> / C <sub>3</sub> H <sub>5</sub> <sup>+</sup>
40 <sup>d</sup>	C <sub>2</sub> H <sub>2</sub> N <sup>+</sup> / C <sub>3</sub> H <sub>4</sub> <sup>+</sup>
39 <sup>dd</sup>	C <sub>2</sub> HN <sup>+</sup> / C <sub>3</sub> H <sub>3</sub> <sup>+</sup>
38	C <sub>3</sub> H <sub>2</sub> <sup>+</sup> / C <sub>2</sub> N <sup>+</sup>
37	C <sub>3</sub> H <sup>+</sup>
36	C <sub>3</sub> <sup>+</sup>
28 <sup>dd</sup>	CH <sub>2</sub> N <sup>+</sup> / C <sub>2</sub> H <sub>4</sub> <sup>+</sup> / CO <sup>+</sup>
27 <sup>d</sup>	<b>C<sub>2</sub>H<sub>3</sub><sup>+</sup></b>

<sup>a</sup> Only peaks which have intensity  $\geq 5\%$  of the m/z 80 peak intensity are listed.

<sup>b</sup> The fragmentation sequence identified in DFT calculations is highlighted in bold (Figs. 5 and 6). For the other channels, all possible product ions are listed apart from those which are strongly counter-intuitive.

<sup>c</sup> Also present as the precursor ion of one or two (<sup>cc</sup>) metastable dissociation bands (see Table 2).

<sup>d</sup> Also present as the product ion of one or two (<sup>dd</sup>) metastable dissociation bands (see Table 2).

**Table 2:** Summary of the metastable band assignments.

Band label <sup>a</sup> in Fig. 3.ii and Fig. 4	m/z of precursor ( $m_i$ ) and product ion ( $m_f$ )	Neutral fragment mass in a.u.	Plausible precursor and product ions <sup>b</sup>
<b>A</b>	<b>109 → 80</b>	<b>29 (HCO)</b>	<b><math>C_6H_7NO^+</math> (3-AP<sup>+</sup>) → <math>C_5H_6N^+</math></b>
B	94 → 66	28	$C_5H_4NO^+$ → $C_4H_4N^+$ / $C_4H_2O^+$ / $C_3NO^+$ $C_6H_6O^+$ → $C_5H_6^+$ / $C_4H_2O^+$
C	92 → 65	27	$C_6H_4O^+$ → $C_4HO^+$ $C_6H_6N^+$ → $C_5H_5^+$ / $C_4H_3N^+$
D	91 → 64	27	$C_6H_5N^+$ → $C_5H_4^+$ / $C_4H_2N^+$
E	82 → 54	28	$C_5H_6O^+$ → $C_4H_6^+$ / $C_3H_2O^+$ $C_4H_4NO^+$ → $C_3H_4N^+$ / $C_3H_2O^+$ / $C_2NO^+$
<b>F</b>	<b>80 → 53</b>	<b>27 (CNH)</b>	<b><math>C_5H_6N^+</math> → <math>C_4H_5^+</math></b>
G	91 → 41	50	$C_6H_3O^+$ → $C_2HO^+$ $C_6H_5N^+$ → $C_2H_3N^+$
H	55 → 54	1	$C_3H_3O^+$ → $C_3H_2O^+$ $C_3H_5N^+$ → $C_3H_4N^+$ $C_4H_7^+$ → $C_4H_6^+$ $C_2HNO^+$ → $C_2NO^+$
I	70 → 43	27	$C_4H_6O^+$ → $C_2H_3O^+$ $C_3H_4NO^+$ → $C_2H_3O^+$ / $CHNO^+$
J	53 → 51	2	$C_3H_3N^+$ → $C_3HN^+$ $C_4H_5^+$ → $C_4H_3^+$
K	69 → 41	28	$C_4H_5O^+$ → $C_3H_5^+$ / $C_2HO^+$ $C_4H_7N^+$ → $C_3H_5^+$ / $C_2H_3N^+$ $C_3H_3NO^+$ → $C_2H_3N^+$ / $C_2HO^+$
L	68 → 40	28	$C_4H_4O^+$ → $C_3H_4^+$ / $C_2O^+$ $C_3H_2NO^+$ → $C_2H_2N^+$ / $C_2O^+$ $C_4H_6N^+$ → $C_3H_4^+$ / $C_2H_2N^+$
M	66 → 39	27	$C_4H_4N^+$ → $C_3H_3^+$ / $C_2HN^+$ $C_5H_6^+$ → $C_3H_3^+$
N	54 → 39	15	$C_3H_4N^+$ → $C_2HN^+$ / $C_3H_3^+$ $C_4H_6^+$ → $C_3H_3^+$
O	69 → 28	41	$C_4H_5O^+$ → $CO^+$ / $C_2H_4^+$ $C_4H_7N^+$ → $CH_2N^+$ / $C_2H_4^+$ $C_3H_3NO^+$ → $CH_2N^+$ / $CO^+$
P	54 → 28	26	$C_3H_4N^+$ → $CH_2N^+$ / $C_2H_4^+$ $C_3H_2O^+$ → $CO^+$ $C_4H_6^+$ → $C_2H_4^+$ $C_2NO^+$ → $CO^+$
<b>Q</b>	<b>53 → 27</b>	<b>26 (C<sub>2</sub>H<sub>2</sub>)</b>	<b><math>C_4H_5^+</math> → <math>C_2H_3^+</math></b>
R	41 → 15	26	$C_2H_3N^+$ → $CH_3^+$ / $NH^+$ $C_3H_5^+$ → $CH_3^+$

<sup>a</sup> The fragmentation sequence identified in DFT calculations is highlighted in bold.

<sup>b</sup> In the absence of calculations or any channels that are strongly counterintuitive, all possible ions are listed.